

Infinite compressibility states in the Hierarchical Reference Theory of fluids.

II. Numerical evidence

Albert Reiner* and Gerhard Kahl

*Institut für Theoretische Physik and Center for Computational Materials Science,
Technische Universität Wien, Wiedner Hauptstraße 8–10, A–1040 Vienna, Austria.*

*e-mail: areiner@tph.tuwien.ac.at

Continuing our investigation into the Hierarchical Reference Theory of fluids for thermodynamic states of infinite isothermal compressibility κ_T we now turn to the available numerical evidence to elucidate the character of the solution of the partial differential equation: of the three scenarios identified previously, only the one following from the assumption of the equations turning stiff when building up the divergence of κ_T allows for a satisfactory interpretation of the data; in addition to the asymptotic regime where the arguments of part I directly apply, a similar mechanism is identified that gives rise to transient stiffness at intermediate cutoff for low enough temperature. Heuristic arguments point to a connection between the form of the Fourier transform of the perturbational part of the interaction potential and the cutoff where finite difference approximations to the differential equation cease to be applicable, and they highlight the rather special standing of the hard-core Yukawa potential as regards the severity of the computational difficulties.

I. INTRODUCTION

In part I [1] of the present series of reports aiming at a characterization of the asymptotic solution of the Hierarchical Reference Theory (HRT, [2–8]) partial differential equation (PDE) for thermodynamic states of diverging isothermal compressibility κ_T a total of three different scenarios have been identified. Sticking to the notational conventions and the definitions introduced in part I, its appendix in particular, these are conveniently distinguished by the values of the exponents r and s in the *ansatzes*

$$\begin{aligned} \frac{\partial f}{\partial Q} &= \mathbf{O}(\bar{\varepsilon}^s), \\ \frac{\partial^2 f}{\partial \varrho^2} &= \mathbf{O}(\bar{\varepsilon}^r) \end{aligned} \quad (1)$$

assumed to hold for large $\bar{\varepsilon}$; here, $f(Q, \varrho)$ is an auxiliary quantity related to the first derivative of the free energy at density ϱ with respect to the renormalization group theoretical cutoff wavenumber Q , and its evolution is governed by a quasi-linear PDE of the form

$$\frac{\partial f}{\partial Q} = d_{00} + d_{02} \frac{\partial^2 f}{\partial \varrho^2}, \quad d_{0i} = \mathbf{O}(\bar{\varepsilon}); \quad (2)$$

integration of this PDE proceeds from $Q = \infty$ all the way to $Q = 0$, thus mirroring the transition from the hard spheres of diameter σ serving as reference system, $v^{(\infty)}(r) \equiv v^{\text{hs}}(r)$, to the physically relevant target system with potential $v^{(0)}(r) \equiv v(r) = v^{\text{hs}}(r) + w(r)$; at intermediate Q , the cutoff dependent potential $v^{(Q)}(r)$ introduced in the derivation of HRT bears little resemblance to $v(r)$ [9] and should be regarded as a purely formal device.

Another auxiliary appearing in the above relations is $\bar{\varepsilon} \equiv \varepsilon - 1$ that is basically the exponential of f ; for the precise definitions of f , $\bar{\varepsilon}$, the PDE coefficients d_{0i} , and any further symbols not explicitly introduced we again refer the reader to part I and its appendix. As shown there, the isothermal compressibility κ_T of the target system is proportional to $\bar{\varepsilon}$ at $Q = 0$ so that infinite compressibility at the critical point and within the binodal directly implies a singular limit of $f(Q, \varrho)$ as $Q \rightarrow 0$; the boundaries of the density range of diverging f are, of course, naturally identified with the densities ϱ_v and ϱ_l of the coexisting vapor and liquid phase. Outside the interval $[\varrho_v, \varrho_l]$, on the other hand, as well as for non-vanishing cutoff at arbitrary density, the solution $f(Q, \varrho)$ of eq. (2) is guaranteed to be continuous and differentiable by construction.

As far as the asymptotic behavior of $f(Q, \varrho)$ for $Q \rightarrow 0$ and $\bar{\varepsilon} \rightarrow \infty$ is concerned, the most natural assumption is that of a smooth solution, corresponding to $r = s = 0$; smoothness as we understand it is tantamount to an $\bar{\varepsilon}$ independence of the Q and ϱ scales characteristic of the variation of f . As discussed in section III of part I, the strongest arguments in favor of this simplistic smoothness assumption are the intuitive appeal of the mechanism sketched there and the prediction $f \propto 1/Q$, immediately implying $r = s = 0$, of the detailed analysis of ref. [7]; these values of the exponents are, however, in direct contradiction with eq. (1) and the asymptotic scaling of the coefficients d_{0i} for large $\bar{\varepsilon}$ so that mathematical consistency can be maintained in this scenario only by taking recourse to an as yet unexplained and hard to accommodate cancellation of terms, *v. i., q. v.* part I.

The other extreme, discussed in section VI of part I, is described by exponents $r > 0$ and $s > 1$; in this case the PDE turns stiff in that part of the integration domain \mathcal{D} where $\bar{\varepsilon}$ is large, and the solution there is characterized by rapid low-amplitude oscillations around the rather slowly varying, large mean value of f . In calculations on discretization grids that maintain a finite separa-

tion of the mesh points even as f and $\bar{\varepsilon}$ diverge, however, these oscillations can neither be followed nor represented numerically so that the solution of the finite difference (FD) approximation to the PDE is bound to reproduce vanishing effective exponents r_{eff} and s_{eff} ; smoothness so having been restored, if only as an artifact of the computational scheme, the arguments of section III B of ref. [7] naturally apply so that $f \propto 1/Q$ is to be expected again numerically even though the markedly non-smooth exact solution of the PDE is likely to display a more rapid average growth, *cf.* sections VI and VII of part I.

In addition to the two scenarios sketched above, referred to as the simplistic, or genuinely smooth one ($r = s = 0$) and the stiff, or only effectively smooth one ($r > 0, s > 1$), respectively, there is also the third possibility of a very weak, *viz.*, logarithmic divergence of f for $Q \rightarrow 0$ ($r = 0, s = 1$): in this case f is a monotonous function of Q wherever $\bar{\varepsilon}$ is large, and $\bar{\varepsilon}Q$ tends to a finite limit for $Q \rightarrow 0$; as we will see, however, the numerical evidence presented in section II clearly rules out such a weak singularity, which is hardly surprising as elimination of the afore-mentioned cancellation is expected to aggravate the divergence of f with respect to that of the smooth solution rather than to reduce it to only a logarithmic one.

It is thus only the simplistic and the stiff scenarios that remain to be considered in the bulk of this report in our attempt to elucidate the true character of the asymptotic solution of the PDE for infinite κ_T . To this end we perform computations on two kinds of model potentials $v(r) = v^{\text{hs}}(r) + w(r)$, *viz.*, on the hard-core Yukawa (HCY) system,

$$w^{\text{hcy}}(r) = \begin{cases} -\epsilon_0 & : r < \sigma \\ -\epsilon \frac{\sigma}{r} e^{-z(r-\sigma)} & : r > \sigma, \end{cases} \quad (3)$$

and on square wells (sws),

$$w^{\text{sw}}(r) = \begin{cases} -\epsilon & : r < \lambda\sigma \\ 0 & : r > \lambda\sigma; \end{cases} \quad (4)$$

a short summary of the parameter sets and of the sample isotherms considered in this study can be found in tab. I.

In both of these potentials, the parameter ϵ coincides with $\lim_{r \rightarrow \sigma^+} (-w(r))$ and so sets the energy scale of the problem; the potential range is given by $1/z$ and $\lambda\sigma$, respectively; and unless stated otherwise, ϵ_0 , the value of $w^{\text{hcy}}(r)$ inside the core, coincides with ϵ , a choice shared with the implementation by the authors of HRT and their coworkers referred to as the original one in ref. [10], *q. v.* section VI. The results of these computations do, indeed, allow us to infer the character of the PDE for subcritical temperatures, $T < T_c$, with great confidence (section III) and so pave the way for some purely heuristic arguments relating the cutoff where smoothing in Q first sets in to the form of the Fourier transform of the perturbational part of the potential (section IV). So having understood the behavior of the PDE in the limit $Q \rightarrow 0$ where asymptotic reasoning valid for large $\bar{\varepsilon}$ applies, we then turn to

similar computationally problematic features of its solution at much higher Q where the numerical evidence points to a mechanism not unlike that at work in the asymptotic region (section V); we close with an informal discussion of the reasons for the atypical computational properties of HCY fluids of moderate inverse screening length z (section VI), postponing practical application of the insight into the solution of the discretized PDE gained thus far to later installments of this series of reports.

II. THE MONOTONICITY ASSUMPTION REFUTED

Of the three scenarios put forward in part I and touched upon in the introduction, the one mentioned last differs markedly from the other two in that the assumption of monotonous growth of f in the asymptotic region allows us to directly infer the merely logarithmic character of its divergence and furnishes the rather specific prediction of $\bar{\varepsilon}Q$ tending to a non-vanishing finite limit for $Q \rightarrow 0$. Of course, $s = 1$ means that, in principle, the smoothing effect discussed in section VI of part I must be reckoned with; the singularity being so mild, however, reduction of $s = 1$ to $s_{\text{eff}} = 0$ is preempted by the standard choice of step sizes ΔQ in the numerical procedure, a choice common to our implementation and the original one:

In the scheme we employ, the cutoff in the i^{th} step of the FD scheme is parametrized as

$$Q_{(i)} = \ln(e^{a-i b} + 1), \quad i = 0, 1, \dots,$$

where a is close to the cutoff $Q_{(0)} \equiv Q_\infty$ where initial conditions are imposed on f ; for large Q , unity may clearly be neglected compared to the exponential so that $Q_{(i)} \rightarrow Q_\infty - i b$, and b is just the spacing $\Delta Q|_\infty$ of successive cutoffs in the large Q limit. For small Q , on the other hand, we have to consider $i \rightarrow \infty$: The exponential then being small, we can apply the first-order expansion $\ln(1+x) = x + \mathbf{O}(x^2)$ to obtain $Q_{(i)} \approx e^{a-i b}$; the step size in Q is then given by

$$Q_{(i+1)} - Q_{(i)} \rightarrow -Q_{(i)} (1 - e^{-b}), \quad Q_{(i)} \rightarrow 0,$$

which is proportional to the cutoff under consideration, $\Delta Q \propto Q$. If $\bar{\varepsilon}Q$ is to approach a constant as predicted by the assumption of monotonous growth these step sizes thus turn out of order $\mathbf{O}(\bar{\varepsilon}^{-1})$, and our discretization should allow us to follow the variation of f reasonably well all the way to $Q = 0$, reproducing a finite limiting value of the product $\bar{\varepsilon}Q$ for $Q \rightarrow 0$. From fig. 1, however, we see that $\bar{\varepsilon}Q$ clearly diverges in this limit; as this finding is corroborated by further calculations with a smaller setting of the numerical parameter $\Delta Q|_\infty$, on finer density grids (down to $\Delta\rho = 5 \cdot 10^{-4}/\sigma^3$), and for both hard-core Yukawa and square well potentials we feel we can safely exclude the monotonous growth scenario from further consideration.

III. SIMPLISTIC SMOOTHNESS VS. STIFFNESS

As for the remaining two alternatives, an attempt to distinguish numerically between genuine and effective smoothness seems doomed at first sight; and indeed, fig. 2 shows the small Q behavior of f within the binodal as obtained numerically to be in excellent agreement with $f \propto 1/Q$, just as predicted by both section III and section VI of part I. In the simplistic scenario, however, mathematical consistency requires an as yet unexplained cancellation, stipulating either that d_{00} turns positive or else that the curvature $\partial^2 f / \partial \varrho^2 < 0$ becomes sufficiently large in modulus to violate the assumption of flatness so essential for the mechanism presumably responsible for the build-up of infinite κ_T (*cf.* section III of part I); as for the former, positive d_{00} is certainly not anticipated on the grounds of eq. (6) of part I nor, in fact, borne out by the numerics; and as far as the purported loss of flatness is concerned, Fig. 2 clearly shows the data obtained in the central part of the density interval $[\varrho_1, \varrho_2]$ (*cf.* fig. 1 of part I) to be hardly distinguishable and the overall variation of f at fixed cutoff Q in the asymptotic regime to be far less than one order of magnitude; in combination with a more detailed look at the data the flatness assumption put forward in section III of part I is clearly confirmed, and we have checked that the situation is largely the same when trading the HCY potential for a SW one, *q. v.* fig. 3, *cf.* section III B below.

In addition to this first indication there are a number of further observations pointing to the smoothness observed being the result of the regularization brought about by insufficient step sizes in the FD equations (FDES) rather than a generic feature of the PDE; indeed, it was our experience with a very careful implementation of HRT [11] that prompted us to consider the possibility of stiffness in the first place.

On a technical level the two candidate solution types differ in the importance to be attributed to the details of the discretization: If, indeed, the PDE turns stiff in the region of large $\bar{\varepsilon}$, reliance on far too large step sizes for subcritical temperatures will generally lead to numerical disaster unless the computational scheme employed stabilizes the integration and so brings about the smoothing discussed in section VI of part I; by way of contrast, a smooth solution like that stipulated in the simplistic scenario should in principle be rather insensitive to the formulation of the problem and the method of discretization; it is revealing that, to the best of our knowledge, no HRT results on simple one-component fluids seem to ever have been obtained for $T < T_c$ except in the quasi-linear formulation of eq. (2) or variants thereof whereas various attempts to directly solve the underlying PDE for a quantity related to the free energy, while fully successful for $T > T_c$, are known to have failed for $T < T_c$ [6,12].

Before turning to more intricate effects encountered numerically and interpreted in terms of the stiff scenario, some general remarks are in place: Letting the labels x

and y refer to either Q or ϱ , smoothing in x sets in at $Q = Q_{\Delta x}$ and can always be postponed, *i. e.*, shifted to lower cutoffs by decreasing the step size Δx ; if, however, the corresponding exponent, r or s , is positive, the rapid growth of f , $\bar{\varepsilon}$ and, by way of eq. (1), of $|\partial^2 f / \partial x^2|$ as the solution proceeds towards $Q = 0$ implies that the amount by which $Q_{\Delta x}$ can be changed in this way and the attendant computational effects must be small; in this case $Q_{\Delta x}$ is thus fairly well defined despite the gradual nature of the transition to the smoothing regime. Furthermore, without loss of generality assuming $Q_{\Delta x} > Q_{\Delta y}$, the solution obtained numerically at cutoffs below $Q_{\Delta x}$ is already affected by smoothing in x so that there is no point in identifying $Q_{\Delta y}$ with the cutoff where Δy becomes too large to describe the variation of the no longer accessible true solution of the PDE; instead, $Q_{\Delta y}$ is taken to be the cutoff where smoothing in y commences in the solution of the FDES, which implies a Δx dependence of $Q_{\Delta y}$ and may even induce $Q_{\Delta y}$ to vanish altogether. For $Q < Q_{\Delta y}$, the solution generated numerically by necessity conforms to the simplistic smoothness assumption as $r_{\text{eff}} = s_{\text{eff}} = 0$ and so grows like $1/Q$; on the other hand, the basic mechanism sketched in section III of part I and the concomitant stabilization of form and monotonicity of f do not explicitly depend on s and thus always set in at $Q_{\Delta \varrho}$. Of course, both $Q_{\Delta Q}$ and $Q_{\Delta \varrho}$ depend on temperature and density, which is taken to be silently accounted for whenever we speak of the form of f at fixed cutoff $Q \leq Q_{\text{smooth}} \equiv \max_x Q_{\Delta x}$. — In numerical applications, the discretized equations generally cannot be solved down to arbitrarily small Q for $T < T_c$; the smallest cutoff attainable on a given discretization grid and at a specific temperature we refer to as Q_{min} ; other than the $Q_{\Delta x}$, Q_{min} cannot depend on ϱ when using predetermined step sizes. Also, the usual way of incorporating the core condition of vanishing pair distribution function for $r < \sigma$ through finite-dimensional matrix-valued ordinary differential equations coupled to the PDE at every point $(Q, \varrho) \in \mathcal{D}$, though perfectly well defined in itself, presents itself as a perturbation of the simplified PDE (2) considered in this report and so may adversely affect the stability of the numerical scheme.

A. Smoothing in ϱ first

As we shall see in a moment, in the case of a hard-core Yukawa fluid of inverse screening length $z = 1.8/\sigma$ already used for fig. 1 the numerics are well compatible with the stiff scenario if only we assume smoothing to occur in the ϱ direction first, $Q_{\Delta \varrho} > Q_{\Delta Q}$. In this case, the mechanism of section III of part I is at work at all cutoffs below Q_{smooth} , guaranteeing small $|\partial^2 f / \partial \varrho^2|$ and stable monotonous growth of f for $\varrho_1 < \varrho < \varrho_2$.

For the moment considering a fixed density grid, the dependence of the results on the step sizes in Q is easily understood: Even though a smaller setting for ΔQ

(or, in our implementation, for the parameter $\Delta Q|_{\infty}$, *v. s.* section II) allows the FDEs longer to mimic the growth of f before switching to $f \propto 1/Q$ at $Q_{\Delta Q}$, as $s > 1 > 0$ the attendant effect on f at fixed density and cutoff $Q < Q_{\Delta Q}$ must be very small. The Q range of sufficient step size leading right up to $Q_{\Delta \varrho}$ where the stabilizing effect linked to smoothing in ϱ sets in, the stability of the FDEs is not an issue and a perturbation of the equations like that brought about by incorporating the core condition in the usual manner is unproblematic. Furthermore, if $f \propto 1/Q$ below $Q_{\Delta Q}$ where $\bar{\varepsilon}$ is large as suggested by ref. [7], section VII of part I, and by fig. 2, the ratio of the f values at two different densities cannot depend on Q and is thus determined by the form of f at the onset of smoothing, *i. e.*, at $Q = Q_{\Delta \varrho}$, alone; given the relative order of the $Q_{\Delta x}$, however, $Q_{\Delta \varrho}$ cannot be affected by ΔQ , and this ΔQ independence of $Q_{\Delta \varrho}$ directly translates into a ΔQ independence of the form of f . As smoothing in ϱ both stabilizes the solution and induces it to grow monotonously, the computation can only fail by way of an overflow due to an insufficient adaptation of the re-scaling of quantities affected by exponentiation of f [10,11], a possibility the likelihood of which is greatly reduced when ΔQ is decreased; correspondingly, larger step sizes are generally accompanied by larger values of Q_{\min} , the smallest cutoff attainable numerically.

Now considering a variation of the density grid, a reduction of $\Delta \varrho$ obviously means that Q_{smooth} is shifted to smaller cutoffs; assuming non-zero r , however, this shift and the attendant effect on f are rather small and $Q_{\Delta \varrho}$ certainly cannot fall below $Q_{\Delta Q}$; consequently, the ratio of f at the onset of smoothing in Q for two different density grids, and the magnitude of the concomitant effect on the final values of f , cannot depend on ΔQ except for roundoff. On the other hand, the ϱ dependence of $Q_{\Delta \varrho}$ indicated in section VI of part I implies a similar density dependence of the amount by which $Q_{\Delta \varrho}$ and the numerical solution for $Q \rightarrow 0$ are affected; a systematic $\Delta \varrho$ dependence of Q_{\min} is not anticipated.

The consequences of assuming the PDE to actually exhibit stiffness for large $\bar{\varepsilon}$ and of $Q_{\Delta \varrho} > Q_{\Delta Q}$ are thus quite specific and therefore open to numerical testing; the simplistic scenario, on the other hand, suggests only a small dependence of the results on ΔQ and $\Delta \varrho$ that should be essentially stochastic in nature, stemming from the truncation error in an otherwise unproblematic FD approximation to the PDE alone.

In tabs. II to IV we summarize the numerical results for a HCY potential with $z = 1.8/\sigma$ obtained on density grids with $\Delta \varrho = 10^{-2}/\sigma^3$ and $\Delta \varrho = 5 \cdot 10^{-4}/\sigma^3$ and varying ΔQ ; the data displayed is, indeed, in full agreement with the above predictions derived from the assumption of stiffness with $Q_{\Delta \varrho} > Q_{\Delta Q}$: For fixed density grid (tabs. II and III, respectively), Q_{\min} and, hence, the final values of f markedly depend on ΔQ , the former generally decreasing and the latter increasing upon reduction of the step size, whereas both the form

of f and its magnitude at fixed cutoff — to be found in the tables under the headings of F_x^y and $f_x Q_{\min} \sigma$, respectively — remain largely unchanged. Comparing the results obtained with different settings for $\Delta \varrho$, on the other hand, the change in the final values of f is indeed almost completely due to the differences in Q_{\min} , whereas the magnitude at fixed Q is affected only moderately, *viz.*, by a few per cent for a twenty-fold increase in the density resolution, and depends on ϱ but not on ΔQ , *cf.* tab. IV. Q_{\min} , on the other hand, is not affected by the density grid in a systematic way, reflecting the probabilistic nature of the process leading to numerical failure of the computation; of the two sample isotherms that founder at comparatively large cutoff, *viz.*, the ones at $\Delta Q|_{\infty} = 0.003/\sigma^3$, $\Delta \varrho = 10^{-2}/\sigma^3$ and at $\Delta Q|_{\infty} = 0.004/\sigma^3$, $\Delta \varrho = 5 \cdot 10^{-4}/\sigma^3$, only the former does not enter the asymptotic regime where $f \propto 1/Q$, as can clearly be seen from tab. IV; as a corollary, for this system and the density grids considered, $Q_{\Delta Q}$ must be sought around $10^{-2}/\sigma$.

B. Smoothing in Q first

In our previous work on HRT we repeatedly stressed the vastly different numerical properties of the HCY and SW potentials, some of the reasons for which will be discussed only in section VI. However, one important factor is our finding that $Q_{\Delta Q}$ exceeds $Q_{\Delta \varrho}$ in SWs, leading to a range of cutoffs $Q_{\Delta \varrho} < Q < Q_{\Delta Q}$ where FDEs are used with inappropriately large step sizes ΔQ while oscillations in ϱ are not yet suppressed and the stabilization wrought by the mechanism of growth first introduced in section III of part I does not make itself felt yet; even though the overall profile of f is expected to resemble fig. 1 of part I, and although $s_{\text{eff}} = 0$, suggesting a general growth proportional to $1/Q$, there is no reason for f to be convex from below throughout the density range $\varrho_1 < \varrho < \varrho_2$; consequently, the sign of $\partial^2 f / \partial \varrho^2$ cannot be known in advance, and episodes of much more rapid variation of f than mere proportionality to $1/Q$ are likely to occur for $Q_{\Delta \varrho} < Q < Q_{\Delta Q}$.

In order to understand how such catastrophic events as can actually be seen from the conspicuous jumps of f evident in fig. 3 may come about, let us consider some cutoffs Q_I and Q_{II} such that $Q_{\Delta \varrho} < Q_I < Q_{II} < Q_{\Delta Q}$, using the subscripts I and II to mark quantities at Q_I and Q_{II} , respectively: As s vanishes effectively, $s_{\text{eff}} = 0$, the slope $\partial f / \partial Q$ is of order $\mathbf{O}(1)$ in $\bar{\varepsilon}$, and so are the increase in f as Q drops from Q_{II} to Q_I and, hence, the ratio f_I / f_{II} . For an essentially $\bar{\varepsilon}$ independent density grid, however, the FD approximation to $\partial^2 f / \partial \varrho^2$, being just a linear combination of f sampled few $\Delta \varrho$ apart, grows in modulus in much the same way as f itself: specifically, the numerical value of $\partial^2 f_I / \partial \varrho^2$ equals $\mathbf{O}(\bar{\varepsilon}_{II}^{\text{eff}}) + \mathbf{O}(\bar{\varepsilon}_{II}^0) f_I / f_{II}$, the second term of which is clearly of order $\mathbf{O}(1)$ in both $\bar{\varepsilon}_I$ and $\bar{\varepsilon}_{II}$; at the same time, $\partial^2 f_I / \partial \varrho^2 = \mathbf{O}(\bar{\varepsilon}_I^{\text{eff}})$ by

definition, and the relation between $\bar{\varepsilon}_I$ and $\bar{\varepsilon}_{II}$ furnished by eq. (A2) of part I directly leads us to conclude that $r_{\text{eff}} = r_{\text{eff}}(f_I \bar{u}_{0,I}^2)/(f_{II} \bar{u}_{0,II}^2)$, *i. e.*, that $r_{\text{eff}} = 0$ in addition to $s_{\text{eff}} = 0$, just as assumed in section III B of ref. [7] where the asymptotic solution proportional to $1/Q$ was first derived. Contrary to the postulates of section III of part I, however, the sign of $\partial^2 f/\partial \varrho^2$ cannot be ascertained, and its magnitude increases in unison with f , *i. e.*, in proportion to $1/Q$; as both d_{00} and d_{02} are of order $\mathbf{O}(\bar{\varepsilon})$ in $\bar{\varepsilon}$, however, the $\mathbf{O}(1)$ growth of $\partial^2 f/\partial \varrho^2$ may well be sufficient to violate the flatness requirement so important for safeguarding the stability of the mechanism of growth discussed in section III of part I at some $Q \in (Q_{\Delta\varrho}, Q_{\Delta Q})$, and rapid variations in f are to be anticipated whenever $|\partial^2 f/\partial \varrho^2|$ becomes too large and so destabilizes the solution.

These catastrophic events of rapid variation of f may, of course, occur at different cutoffs for different densities, most often close to the edges ϱ_1 and ϱ_2 of the region of large f where the $Q_{\Delta x}$ are smallest, and in principle they should lead to both increases and decreases in f ; considering the numerics, however, a marked decrease is almost certain to bring the calculation to an end, whereas rather mild jumps to larger f may relax the relative curvature of f to the point of allowing the solution to enter once more an episode of near-stability characterized by growth in approximate proportion to $1/Q$. In addition to the overflows triggered by either an insufficient adaptation of the rescaling of $\mathbf{O}(\bar{\varepsilon})$ quantities already mentioned in section III A or by a sudden increase in f there is thus a further mode of failure of the computation when a jump to smaller values of f and $\bar{\varepsilon}$ actually renders $\varepsilon = \bar{\varepsilon} + 1$ negative, corresponding to complex f and free energy. As for the incorporation of the core condition into the equations, any such perturbation is likely to exacerbate the risks associated with deviations from proportionality to $1/Q$, though of course we expect the effect of the core condition to be smaller for longer ranged potentials; in this context it may be of interest that our previous work on SWS showed the critical point to be accessible for a wider range of the potential parameter λ when restricting the expansion of the direct correlation function inside the core to a smaller number of basis functions, *cf.* section IV E of ref. [13], *q. v.* appendix E of ref. [12].

Turning to the discussion of the significance of the step sizes ΔQ and $\Delta \varrho$ for the numerical results, the precarious nature of the stability of the computation certainly allows us to interpret the SW data summarized in tabs. V and VI: First of all, the basic mechanism governing the evolution of f in the asymptotic region is linked to too large ΔQ , whereas the density grid is still adequate for representing the ϱ dependence of the solution of the elliptic boundary value problem to be solved at any cutoff Q ; if the numerical process were stable, there should thus be no appreciable dependence of the results on $\Delta \varrho$; in the absence of the stabilization wrought by smoothing in ϱ , however, even the small differences seen upon variation

of $\Delta \varrho$ must be expected to shift the episodes of rapid evolution to slightly different cutoffs, though in an unsystematic way. Recalling that Q_{min} itself is most likely the location of an attempted jump in f that leads to the termination of the computation, the non-monotonous dependence of Q_{min} on the step sizes evident from tabs. V and VI is easy to understand: as expected in the stiff scenario with $Q_{\Delta Q} > Q_{\Delta \varrho}$, a pronounced ΔQ dependence is accompanied by only a very modest effect as $\Delta \varrho$ is varied, even though the relative change in $\Delta \varrho$ between the tables is much larger than the ΔQ range covered. As far as the final form of f is concerned, different ΔQ should leave it unaltered as long as the number and, at least approximately, the positions of the jumps do not change, and the $\Delta \varrho$ dependence should be small again; sure enough, this is exactly what is to be seen from the entries in the tables under headings of the form F_x^y ; of course, $Q_{\Delta \varrho}$ being monotonous in f the jumps are to be expected to occur close to ϱ_1 and ϱ_2 most often, as is immediately evident from fig. 3, which is also the reason why we have chosen to present the ratios of neighboring densities rather than always referring to the data at one and the same density as has been the case in tabs. II and III.

One last point worth mentioning regards the possibility of jumps leading to smaller values of f : Indeed, the top entry of tab. V has negative f , corresponding to $\varepsilon = \bar{\varepsilon} + 1 \sim 10^{-27}$ that is the result of a downward jump from $f \sim +10^4$ ($\varepsilon \sim 10^{5000}$) at only slightly higher cutoff where the form of f again resembles that stipulated in section III, and sketched in fig. 1, of part I; considering the FDES, it is clear that even a minor perturbation might well have led to negative ε so that no real solution f to the equations would have been found; in this case the last step would have been discarded by our program, and the final results reported would once more conform with the patterns discernible in the remainder of the data as discussed above.

Of course, due to the vagaries of a numerical process always on the brink of losing stability — an issue that should be clearly distinguished from the question of the stability of the PDE itself —, our predictions in the present section are somewhat less specific than in section III A; still, the observed trends are in good agreement with our expectations: needless to say, the mere existence of the catastrophic events so characteristic of the numerical process are in direct contradiction to the simplistic scenario that, furthermore, would be hard pressed to provide so much as a hint to the cause of the different degrees of sensitivity of the results to variations of ΔQ and $\Delta \varrho$, respectively. All in all, the assumption of the observed smoothness of the numerical solution $f(Q, \varrho)$ being brought about by discretization of a carefully chosen formulation of a stiff PDE on too coarse a grid provides us with a means of interpreting trends seen numerically that can hardly be accounted for in the simplistic scenario; from now on we will therefore take it for granted that the PDE for f must, indeed, be characterized as stiff

in that part of its domain \mathcal{D} where the infinite isothermal compressibility κ_T is built up as fluctuations on ever larger lengthscales are taken into account; this point of view is further corroborated by the effects discussed in section IVE of ref. [13] as well as in section V of the current report.

IV. THE ONSET OF SMOOTHING IN Q

If this view of the underlying PDE and the numerical process by which an approximate solution is sought is correct, it is natural to inquire into the typical values of the cutoffs $Q_{\Delta x}$ where smoothing in x sets in; although we are currently in no position to even tentatively predict the location of $Q_{\Delta \varrho}$ from the properties of the model system under consideration, in the following we present some purely heuristic arguments that may be credited with shedding some light on the factors that influence the value of $Q_{\Delta Q}$; as the exponents r and s are non-vanishing by assumption, the $Q_{\Delta x}$ may only weakly depend on the discretization grid and are thus largely determined by the perturbational part of the potential alone.

In order to extract a likely position of $Q_{\Delta Q}$ from the PDE we consider a thermodynamic state of diverging isothermal compressibility at a cutoff that is low enough for smoothing in Q to have set in at least partially, $Q \lesssim Q_{\Delta Q}$: taking into account the gradual transition between the smoothing and non-smoothing regimes, the effective exponent s_{eff} may not vanish exactly yet; nevertheless it seems safe to assume $s_{\text{eff}} < 1$. Let us now define an auxiliary quantity $\psi(Q, \varrho)$ through the relation

$$\tilde{\mathcal{K}} + \psi \tilde{u}_0 = -\frac{\tilde{\varepsilon}}{\tilde{\phi}}; \quad (5)$$

in the notation of our earlier work on HRT [10,12,13] ψ corresponds to $\tilde{\phi}_0 + \gamma_0$, where γ_0 is an expansion coefficient in the *ansatz* for the direct correlation function that is used to enforce thermodynamic consistency in the form of eq. (A5) of part I. Solving the above relation for ψ and differentiating once with respect to Q we find

$$\frac{\partial \psi}{\partial Q} = -\tilde{\phi}_0 \left(\frac{\partial}{\partial Q} \frac{1}{\tilde{\varepsilon}} + \frac{\partial}{\partial Q} \frac{\tilde{\mathcal{K}}}{\tilde{\phi}} \right),$$

which, of course, is not valid close to the zeros $Q_{\tilde{\phi},i}$ of $\tilde{\phi}$ and \tilde{u}_0 where eq. (5) cannot be inverted to yield ψ . As shown in section 2.4.1 of ref. [12], the compressibility sum-rule also allows one to derive a PDE for γ_0 that is equivalent to eq. (2) itself; taking into account the density independence of the potential we easily find that the evolution of ψ is given by

$$\begin{aligned} \frac{\partial \psi}{\partial Q} &= -\frac{Q^2}{4\pi^2} \frac{\partial^2}{\partial \varrho^2} \ln \varepsilon \\ &= \frac{Q^2}{4\pi^2} \left(-\tilde{u}_0^2 \frac{\partial^2 f}{\partial \varrho^2} + \tilde{\phi} \frac{\partial^2}{\partial \varrho^2} \frac{1}{\tilde{\mathcal{K}}} \right). \end{aligned}$$

Equating the two expressions for $\partial \psi / \partial Q$ we can now solve for $\partial^2 f / \partial \varrho^2$ and insert the result into eq. (2) to obtain the rate of change of f as

$$\frac{\partial f}{\partial Q} = d_{00} + \frac{d_{02} 4\pi^2}{Q^2 \tilde{u}_0^2} \left(\tilde{\phi}_0 \frac{\partial}{\partial Q} \frac{1}{\tilde{\varepsilon}} + \frac{\partial}{\partial Q} \frac{\tilde{\mathcal{K}}}{\tilde{u}_0} \right) + \frac{d_{02} \tilde{\phi}_0}{\tilde{u}_0} \frac{\partial^2}{\partial \varrho^2} \frac{1}{\tilde{\mathcal{K}}} \quad (6)$$

for Q away from the $Q_{\tilde{\phi},i}$; of course, both d_{00} and d_{02} are negative in the case under consideration.

For smoothing in Q to set in we expect f to be large already in the sense of $\tilde{\varepsilon} \gg f$, or else reasoning based on the asymptotic behavior for large $\tilde{\varepsilon}$ is inapplicable; furthermore, recalling the definition of $Q_{\Delta x}$ as that value of the cutoff where the step sizes Δx become insufficient for representing the variation of the solution of the PDE it is plausible that $Q_{\Delta Q}$ should be located close to where the slope $-\partial f / \partial Q$ of f is rather large; at the same time, the reference system being fixed, $Q_{\Delta Q}$ can only depend on the form of the Fourier transform of the perturbational part of the interaction potential, *i. e.*, on $\tilde{u}_0 = \tilde{\phi} / \tilde{\phi}_0$ rather than on $\tilde{\phi}$ itself: the temperature $T = 1/k_B \beta$ enters the calculation only as a pre-factor to the interaction potential, *viz.*, through $\phi = -\beta w$ so that the normalization of $\tilde{\phi}$ only fixes an energy or temperature scale.

With this in mind we return to eq. (6): Of the expressions appearing on its right hand side the one involving the Q derivative of $1/\tilde{\varepsilon}$ is of order $\mathbf{O}(\tilde{\varepsilon}^{s_{\text{eff}}-1})$ in $\tilde{\varepsilon}$ and so can be neglected if f is large and $s_{\text{eff}} < 1$ as assumed; and as we are looking for an effect triggered by the form of $\tilde{\phi}$ alone we do not have to consider the derivatives of the properties of the hard sphere reference system encoded in $\tilde{\mathcal{K}}$. Consequently, it is the term involving the Q derivative of \tilde{u}_0 that is of interest to us in the first place: noting the ideal gas contribution $-1/\varrho$ to $\tilde{\mathcal{K}}$ that ensures positive $d_{02} \tilde{\mathcal{K}}$ we find that the relevant term is the product of $\partial \tilde{u}_0 / \partial Q$ and manifestly positive factors. Now assume that $Q_{\Delta Q}$ is less than the position of the first minimum of \tilde{u}_0 so that only the monotonous growth of \tilde{u}_0 towards its global maximum at $Q = 0$ remains to be covered by the solution of the PDE: clearly, as the calculation proceeds in the negative Q direction, the steeper this rise of \tilde{u}_0 , the more the $\partial \tilde{u}_0 / \partial Q$ term counteracts the growth of f , thereby effectively further delaying the onset of smoothing in Q ; most likely, $Q_{\Delta Q}$ will thus be found at cutoffs so low that \tilde{u}_0 already levels off towards its limiting value of unity. Even a superficial glance at \tilde{u}_0 for two typical potentials, *viz.* the HCY system with $z = 1.8/\sigma$ (solid curve) and SWs (dashed curve) as displayed in fig. 4 shows that, for these systems, \tilde{u}_0 levels off when Q (or λQ , in the case of SWs) is no more than a few $10^{-1}/\sigma$, which is certainly not in contradiction to the estimate presented at the end of section III A, especially in the light of section VI below; on the other hand, figs. 2 and 3 demonstrate that the transition to the regime where f mostly grows like $1/Q$ occurs at similar values of the cutoff; as this type of solution corresponds to a vanishing effective exponent

s_{eff} this transition is likely to be a good indicator for the onset of smoothing in Q . All in all, we are thus led to expect that either $Q_{\Delta Q}$ is larger than the position of the first minimum of \tilde{u}_0 , the case not considered above, or else that $Q_{\Delta Q}$ should be located at a much smaller cutoff, *viz.*, where \tilde{u}_0 is already close to unity and $|\text{d}\tilde{u}_0/\text{d}Q|$ is small; it is the latter of these possibilities that is in accordance with the data displayed in figs. 2 and 3 and the tables referenced earlier so that our arguments, heuristic as they are, do indeed seem to provide us with a means of estimating $Q_{\Delta Q}$ in a satisfactory way. Unfortunately, the location of $Q_{\Delta Q}$ so far eludes determination from the potential alone by a comparably simple line of thought, and actual numerical solution of the PDE currently is the only way of studying $Q_{\Delta Q}(T, \varrho)$ available to us.

V. BEYOND ASYMPTOTICS

So having arrived at a basic understanding of the relation between the Fourier transform $\tilde{w} \propto \tilde{\phi} \propto \tilde{u}_0$ of the perturbational part of the potential and the cutoff $Q_{\Delta Q}$ where the step sizes in Q are no longer compatible with the rate of change of f and so bring about smoothing in Q , one might expect numerical difficulties linked to the discretization grid to first surface at about the same cutoff, *viz.*, around $Q \sim 10^{-1}/\sigma$ for the potentials considered earlier. However, the monitoring variant of our code [10–12] that must be credited with first highlighting and bringing to our attention the purported stiffness of the equations clearly signals the inadequacy of number and spacing of the vertices in the FDES at much higher cutoff, *viz.*, typically for $5 < Q\sigma < 10$: indeed, the asymptotic region of large $\bar{\varepsilon}$ can never even be reached without renouncing control of the local truncation error in solving the equations since otherwise the step sizes appropriate in FD calculations would render the results of fixed precision floating point operations insignificant, *cf.* section III E of ref. [10]. In combination with the observed patterns of the evolution of f at intermediate and small Q illustrated in figs. 2, 3, and 5, our experience with the numerics of HRT leads us to propose the existence within the domain of the PDE of several regions of large f where phenomena similar to those discussed before are to be reckoned with; in particular, the PDE may turn stiff not only in the asymptotic region but also at higher cutoff. While the existence of patches of large f adjacent to the high density boundary at intermediate Q is quite apparent from fig. 5, other than in part I we do not have at our disposal the guarantees of unboundedness and continuity of f that ensure the validity of conclusions drawn from the asymptotic behavior of the various terms in the PDE for large $\bar{\varepsilon}$ alone, and the small value of \tilde{u}_0^2 evident from fig. 4 further complicates the situation in that $\bar{\varepsilon}$ may not be large compared to f even if $f \gg 1$; still, from eqs. (A1) and (10) of part I we see that d_{02} is negative and appreciable for all Q in the cutoff range we are interested in

except very close to the $Q_{\tilde{\phi},i}$ and that d_{00} is likely to be rather large in modulus, although it is the terms linear in f rather than those involving $\bar{\varepsilon}$ that are of prime importance now. It is then conceivable that in some parts of the domain \mathcal{D} of the PDE — following the reasoning of section IV and considering eq. (A1) of part I, the signs of $\tilde{\phi}$ and of its slope are anticipated to play an important *rôle* in locating these — f may become large and, by way of the d_{0i} behavior there, prompt rapid further growth as Q proceeds to smaller values, effectively mandating either impractically small step sizes ΔQ or else deliberate resignation of bounded local truncation errors, *v. s.*; on the other hand, just as in section III B such a rapid growth of f is almost certainly accompanied by a similar growth of $|\partial^2 f/\partial \varrho^2|$ on the grid, and the oscillatory nature of this curvature is likely to carry over to $\partial f/\partial Q$, too: qualitatively the situation during these episodes of rapid evolution is thus quite similar to the stiff scenario, and it seems reasonable to surmise that this might be the reason for the inability of a numerical scheme insisting on local convergence and appropriateness of the dynamically adjusted discretization mesh to ever enter the asymptotic region of large $\bar{\varepsilon}$; at the same time these considerations clarify why the lowest temperature attainable numerically, denoted $1/k_B\beta_{\text{max},\#}$ in refs. [12,13] may well be higher than T_c even though stiffness in the asymptotic region is a problem only for $T \leq T_c$, *v. i.*

Without the backing of more formal arguments much of the above line of thought may seem insubstantial and might thus be viewed with suspicion; there are, however, a number of numerical effects that provide at least indirect evidence for the point of view just laid out; among those that have already been identified and discussed in our earlier work on HRT, the plummeting step sizes observed when determining the discretization grid from the local curvature of appropriate components of the solution vector [10,11] are a telltale sign of the inappropriateness of the predetermined ΔQ detailed in section II and so provide the most direct evidence for the interpretation of the numerics at intermediate Q in terms of stiffness of the PDE in part of \mathcal{D} , *v. s.*; we should also mention the peculiar shifts in the critical temperature seen for square well fluids whenever the potential range parameter λ is close to a simple fraction, an effect linked to the modulation of $\bar{\varepsilon}$ by the interference of \tilde{c}_2^{ref} and $\tilde{\phi}$ [13]. Further support comes from the observation that isotherms at the lowest temperatures attainable numerically show no sign of phase separation if $\beta_{\text{max},\#} < \beta_c$ (the critical temperature being known independently from related computations or by other methods), thereby ruling out an unfortunate slip of the critical temperature in combination with the stiffness in the asymptotic region as the cause for the failure to converge towards $Q = 0$ for β only slightly above $\beta_{\text{max},\#}$. The vestiges of stiffness at intermediate cutoff are also to be seen from the interplay of the $Q_{\tilde{\phi},i}$ with the boundaries of the Q intervals affected by smoothing that manifests itself in the width of the

two-phase region; just as the reaction of the binodal to a local density grid refinement, however, this issue cannot be discussed without reference to the details of the data analysis in the presence of non-uniform high-resolution density grids and will thus be dealt with only in part III [14].

VI. HARD CORE YUKAWA VS. OTHER POTENTIALS

By now we have arrived at what we feel to be as satisfactory an understanding of the numerical process as can be expected from considerations as summary in character as those put forward in part I and in the preceding section V of the present contribution; according to our perception of the evolution of the solution of the PDE, numerical problems due to inappropriateness of a discretization grid maintaining a practical separation of the vertices throughout the integration domain \mathcal{D} must be anticipated for low enough temperature both as the divergence of the isothermal compressibility κ_T is built up for $Q \rightarrow 0$ and at much larger cutoff when the PDE temporarily turns stiff in isolated patches of \mathcal{D} ; further sources of difficulties like, *e. g.*, the initial and high-density boundary conditions or the implementation of the core condition have been discussed extensively elsewhere [10,12,13].

Throughout our numerical work, however, we consistently found that HCY fluids of moderate inverse screening length like, *e. g.*, the one with $z = 1.8/\sigma$ repeatedly used in this report exhibit all these phenomena only in a rather mild form; for $Q \rightarrow 0$ this is, indeed, to be expected from the stiff scenario if only we accept the in itself unexplained finding of $Q_{\Delta\varrho} > Q_{\Delta Q}$, whereas the merely qualitative considerations of section V do not allow us to directly tackle the problem of clarifying the computational benignity of HCYs at intermediate Q . Both the relative order of $Q_{\Delta Q}$ and $Q_{\Delta\varrho}$ in the asymptotic region and the comparable innocuousness of the stiffness at higher cutoff seem, however, to be linked to a specific feature of the form of the Fourier transform of the perturbational part of the interaction potential:

Once more considering fig. 4 we immediately find that the HCY \tilde{u}_0 with the default choice of $\epsilon_0 = \epsilon$ differs quite markedly from the curve obtained for SWs in that the local extrema of \tilde{u}_0 at $Q > 0$ are rather small in modulus, as can also be seen from the numbers quoted in the caption to fig. 4. It is easily checked that the special standing of the default HCY system in this regard remains unchallenged even for other parameters and types of potentials: the main difference between SWs and other short-ranged non-HCY potentials like, *e. g.*, Lennard-Jones systems concerns the phase of the swings of \tilde{u}_0 , *i. e.*, the location rather than the size of the local extrema; and although an increase in z , corresponding to a shorter ranged HCY system, can be shown to reduce the slope of \tilde{u}_0 and to

enhance the local extrema, the effect is quite small for moderate screening length and approaches the SW case only in the limit $z \rightarrow \infty$ that actually transforms v^{hcy} into a SW potential of vanishing well width, $\lambda = 1$.

As for the first of the questions laid out above, *viz.*, the reason for $Q_{\Delta Q}$ being less than $Q_{\Delta\varrho}$, let us shortly return to section IV, recalling the decisive *rôle* played by the steepness of \tilde{u}_0 as it rises to its global maximum in fixing $Q_{\Delta Q}$: If it is really this final rise of \tilde{u}_0 towards unity that suppresses the onset of smoothing in Q and so determines the value of $Q_{\Delta Q}$ as per the arguments of section IV, the question arises by what standard the slope is to be judged: the short rangedness of the potential notwithstanding, the PDE surely cannot sense the volume integral and global normalization of $\tilde{\phi}$ that only serve to set an energy and temperature scale, which rules out the possibility of the absolute value of the slope lying at the heart of the question; instead, it is natural to assume that it is the variation of \tilde{u}_0 seen at larger Q relative to which the steepness must be assessed. The above considerations then show quite clearly that the HCY potential with $\epsilon_0 = \epsilon$ displays a particularly prominent rise *vis-à-vis* the amplitudes of its oscillations at higher cutoff, conceivably leading to especially small $Q_{\Delta Q}$ that so falls below $Q_{\Delta\varrho}$, *q. v.* sections III A and IV.

By the same token we can also understand the computational properties of HCY fluids at intermediate cutoff: For every one of the patches of potential stiffness including the asymptotic region there is an associated temperature above which computational problems prevent bounded local truncation errors on practical discretization grids while the FD equations may still admit a numerical solution; for small cutoff, these difficulties are linked to the build-up of the divergence of the isothermal compressibility, the relevant temperature coincides with T_c , and for $T > T_c$ there is never any form of stiffness as attested by, *e. g.*, ref. [6] as well as our own numerical experience [12]. However, as the temperature enters the calculation only *via* $\tilde{\phi}$, the only measure of temperature available to the PDE before entering the asymptotic region is the amplitude of the undulations of $\tilde{\phi}$ so that the particularly small local extrema encountered in the HCY fluid effectively render the numerics at intermediate cutoff similar to what would be found only at much higher T/T_c in other systems, thus reducing the problem posed by stiffness there.

Supposing the above line of thought to actually capture the very reason for the singular position of the default choice of HCY potential, our interest is naturally drawn to the form of \tilde{u}_0 and, therefore, to the choice of $w(r)$ inside the core: after all, with hard spheres serving as reference system the splitting of the full interaction potential v into v^{ref} and w is not uniquely determined for $r < \sigma$, and different choices for $w(r)$ there necessarily yield different $\tilde{\phi}$, which immediately carries over to f and all the other properties of the Q system for every non-vanishing Q ; physically meaningful quantities,

on the other hand, obviously should not be affected in the limit $Q \rightarrow 0$, an expectation that is actually borne out numerically in some preliminary calculations on the Girifalco description of fullerenes in a rather satisfactory way. Indeed, the continuation of $w(r)$ inside the core plays a vital *rôle* for the local extrema: as exemplified by the dot-dashed curve in fig. 4 corresponding to the HCY potential with $\epsilon_0 = 0$ any discontinuity in $w(r)$ at $r = \sigma$ is bound to feature prominently in the Fourier transform, and even a moderate deviation from the standard choice of $\epsilon_0 = \epsilon$ renders the local extrema of \tilde{u}_0 comparable to those seen for SWS, causing massive numerical difficulties at intermediate Q similar to those found in SWS [10,12]. On the other hand, if we not only avoid such a discontinuity but rather extend the Yukawa form all the way to the origin — hardly an unproblematic choice in our formulation as it entails diverging direct correlation function at $r = 0$ and invalidates the expansion method of taking into account the core condition [6] —, Fourier transformation yields $\tilde{u}_0(Q) = z^2/(z^2 + Q^2)$ which is positive and strictly monotonous for all Q (dotted curve in fig. 4); the properties of \tilde{u}_0 pointed out before and the attendant especially attractive numerical properties of HCY fluids with the standard setting of ϵ_0 can thus be traced back to a particular choice of $w(r)$ for $r < \sigma$ in the definition of eq. (3) and so are no genuine traits of this model system. Heuristic as the considerations of this section are, they clearly confirm the finding of deteriorating accuracy of HRT for narrower potentials — a problem that certainly cannot be discussed without a detailed inquiry into the deficiencies of the usual implementation of the core condition — as reported in ref. [15] where HCY potentials of inverse screening length in the range $1.8/\sigma \leq z \leq 9/\sigma$ were considered; at the same time, they also caution against general conclusions on the merits of HRT relative to those of other thermodynamically consistent liquid state theories on the basis of work done on HCY potentials alone. The alleged influence of the form of $\tilde{\phi}$ on the severity of the numerical difficulties encountered when solving the HRT-PDE also opens up the possibility of tuning the computational properties of some given potential by optimizing $w(r)$ inside the core in such a way that the local extrema are reduced in magnitude, an avenue largely unexplored to date the merit of which we are currently in no position to assess.

With these rather informal and partly speculative considerations the present installment of this short series of reports on the character and essential features of the HRT-PDE for thermodynamic states of infinite isothermal compressibility κ_T draws to an end: following the rather summary analysis of the PDE based upon the behavior of its coefficients d_{0i} in the limit of large $\bar{\epsilon}$ presented in part I, by now we have not only managed to rule out two of the three scenarios formulated there, demonstrating that the numerical evidence admits a satisfactory interpretation within the framework furnished by the assumption of stiffness in the asymptotic region, but we have also succeeded in extending some of our conclusions to similar

effects at intermediate cutoff Q ; all in all, we feel that we have amassed a considerable amount of numerical experience and arrived at a rather detailed and self-consistent perception of the computational process all the way from the initial conditions imposed at large Q to the final results at $Q = 0$ where the solution reproduces the singularity of κ_T at the critical point or at phase coexistence. Needless to say, given the precarious nature of the HRT numerics and the not altogether unproblematic relation between the PDE and the FD approximation to it such an understanding is of prime importance if systematic mistakes are not to be introduced into the results unknowingly; we will strive to bring to fruition our concept of the integration of the discretized equations in part III [14] where we will also discuss the significance of our findings so far on the data analysis, an endeavour that seems all the more worthwhile in view of the high promise of HRT as one of the few theories of the liquid state that remain applicable even in the critical region.

VII. ACKNOWLEDGMENTS

The authors gratefully acknowledge financial support from *Fonds zur Förderung der wissenschaftlichen Forschung* under project number 15758.

-
- [1] A. Reiner, *Infinite compressibility states in the hierarchical reference theory of fluids. I. Analytical considerations*, submitted to J. Stat. Phys.. Available on the world wide web from <http://purl.oclc.org/NET/a-reiner/sci/texts/20030615-0/>.
 - [2] A. Parola, L. Reatto, *Liquid state theories and critical phenomena*, Adv. Phys. **44**, 211–298 (1995).
 - [3] A. Parola, L. Reatto, *Liquid-state theory for critical phenomena*, Phys. Rev. Lett. **53**, 2417–2420 (1984).
 - [4] A. Parola, L. Reatto, *Hierarchical reference theory of fluids and the critical point*, Phys. Rev. A **31**, 3309–3322 (1985).
 - [5] A. Parola, A. Meroni, L. Reatto, *Comprehensive theory of simple fluids, critical point included*, Phys. Rev. Lett. **62**, 2981–2984 (1989).
 - [6] A. Meroni, A. Parola, L. Reatto, *Differential approach to the theory of fluids*, Phys. Rev. A **42**, 6104–6115 (1990).
 - [7] A. Parola, D. Pini, L. Reatto, *First-order phase transitions, the Maxwell construction, and the momentum-space renormalization group*, Phys. Rev. E **48**, 3321–3332 (1993).
 - [8] M. Tau, A. Parola, D. Pini, L. Reatto, *Differential theory of fluids below the critical temperature: Study of the Lennard-Jones fluid and of a model of C₆₀*, Phys. Rev. E **52**, 2644–2656 (1995).

- [9] A. Reiner, G. Kahl, Poster presented at *5th EPS Liquid Matter Conference*, Konstanz, Germany, 2002. Abstract in *Europh. Conf. Abs.* **26F**, 10.17 (2002). Available on the world wide web from <http://purl.oclc.org/NET/a-reiner/sci/texts/20020915-0/>.
- [10] A. Reiner, G. Kahl, *Implementation of the hierarchical reference theory for simple one-component fluids*, *Phys. Rev. E* **65**, 046701 (2002). E-print [cond-mat/0112035](http://arxiv.org/abs/cond-mat/0112035).
- [11] A. Reiner, *ar-HRT-1*. Available on the world wide web from <http://purl.oclc.org/NET/ar-hrt-1/>.
- [12] A. Reiner, *The hierarchical reference theory. An application to simple fluids*, PhD thesis, Technische Universität Wien (2002). Available on the world wide web from <http://purl.oclc.org/NET/a-reiner/dr-thesis/>.
- [13] A. Reiner, G. Kahl, *The hierarchical reference theory as applied to square well fluids of variable range*, *J. Chem. Phys.* **117**, 4925–4935 (2002). E-print [cond-mat/0208471](http://arxiv.org/abs/cond-mat/0208471).
- [14] A. Reiner, G. Kahl, *Infinite compressibility states in the hierarchical reference theory of fluids III*, in preparation. Available on the world wide web from <http://purl.oclc.org/NET/a-reiner/sci/texts/20030710-0/>.
- [15] C. Caccamo, G. Pellicane, D. Costa, D. Pini, G. Stell, *Thermodynamically self-consistent theories of fluids interacting through short-range forces*, *Phys. Rev. E* **60**, 5533–5543 (1999).

system	$\beta_c \epsilon$	$\varrho_c \sigma^3$	$\beta \epsilon$	$\varrho_v \sigma^3$	$\varrho_l \sigma^3$
sw, $\lambda = 3$	0.1011	0.26(1)	0.115	0.075(5)	0.510(5)
HCY, $z = 1.8/\sigma$	0.8316	0.33(1)	0.875	0.145(5)	0.525(5)

TABLE I. Overview of systems and sample isotherms: The locus of the critical point and the extent of the two-phase region for the isotherms underlying the tables and figures of the present contribution as obtained from HRT calculations not imposing the core condition. All of the digits given for β_c are significant.

$\Delta Q \Big _{\infty} \sigma$	$Q_{\min} \sigma$	$f_{0.2}$	$f_{0.2} Q_{\min} \sigma$	$F_{0.2}^{0.3}$	$F_{0.2}^{0.4}$	$F_{0.2}^{0.5}$
0.003	$9.914 \cdot 10^{-3}$	$3.643 \cdot 10^2$	3.612	1.862	1.755	0.590
0.004	$3.995 \cdot 10^{-5}$	$8.990 \cdot 10^4$	3.592	1.867	1.758	0.585
0.005	$5.014 \cdot 10^{-5}$	$7.163 \cdot 10^4$	3.592	1.867	1.758	0.585
0.010	$9.943 \cdot 10^{-5}$	$3.612 \cdot 10^4$	3.592	1.867	1.758	0.585

TABLE II. ΔQ dependence of the final results for a hard-core Yukawa system: Just as in figs. 1 and 2, $z = 1.8/\sigma$, $\beta = 0.875/\epsilon$, and $\Delta \varrho = 10^{-2}/\sigma^3$; we use the notation f_x for $f(Q_{\min}, x/\sigma^3)$ and define $F_x^y = f_y/f_x$.

$\Delta Q \Big _{\infty} \sigma$	$Q_{\min} \sigma$	$f_{0.2}$	$f_{0.2} Q_{\min} \sigma$	$F_{0.2}^{0.3}$	$F_{0.2}^{0.4}$	$F_{0.2}^{0.5}$
0.003	$3.131 \cdot 10^{-5}$	$1.167 \cdot 10^5$	3.652	1.865	1.768	0.625
0.004	$1.004 \cdot 10^{-2}$	$3.638 \cdot 10^2$	3.653	1.865	1.768	0.625
0.005	$5.014 \cdot 10^{-5}$	$7.285 \cdot 10^4$	3.652	1.865	1.768	0.625
0.010	$1.004 \cdot 10^{-4}$	$3.637 \cdot 10^4$	3.653	1.865	1.768	0.625

TABLE III. ΔQ dependence of the final results for a hard-core Yukawa system: The parameters and notation coincide with those of tab. II, except for $\Delta \varrho = 5 \cdot 10^{-4}/\sigma^3$.

$\Delta Q \Big _{\infty} \sigma$	$G_{0.2}$	$G_{0.3}$	$G_{0.4}$	$G_{0.5}$
0.003	1.011	1.013	1.018	1.072
0.004	1.017	1.016	1.022	1.087
0.005	1.017	1.016	1.022	1.086
0.010	1.017	1.016	1.022	1.086

TABLE IV. $\Delta \varrho$ dependence of the form of the final results for a hard-core Yukawa system at varying ΔQ : The parameters coincide with those of tabs. II and III; perusing the notation introduced there, G_x is $f_x Q_{\min} \sigma$ as evaluated for $\Delta \varrho = 5 \cdot 10^{-4}/\sigma^3$ divided by the same quantity for $\Delta \varrho = 10^{-2}/\sigma^3$.

$\Delta Q \Big _{\infty} \sigma$	$Q_{\min} \sigma$	$f_{0.15}$	$F_{0.15}^{0.25}$	$F_{0.25}^{0.35}$	$F_{0.35}^{0.45}$
0.003	$4.181 \cdot 10^{-4}$	$-1.415 \cdot 10^5$	2.379	1.635	0.392
0.004	$3.198 \cdot 10^{-4}$	$3.597 \cdot 10^4$	1.589	0.965	0.523
0.005	$3.318 \cdot 10^{-4}$	$3.465 \cdot 10^4$	1.589	0.965	0.523
0.010	$3.576 \cdot 10^{-4}$	$3.225 \cdot 10^4$	1.589	0.965	0.523

TABLE V. ΔQ dependence of the final results for a sw system with $\lambda = 3$, $\beta = 0.115/\epsilon$, and $\Delta \varrho = 10^{-2}/\sigma^3$; we use the same notation as in tab. II.

ΔQ	σ	$Q_{\min} \sigma$	$f_{0.15}$	$F_{0.15}^{0.25}$	$F_{0.25}^{0.35}$	$F_{0.35}^{0.45}$
0.003		$4.206 \cdot 10^{-4}$	$2.812 \cdot 10^4$	1.584	0.974	0.547
0.004		$3.302 \cdot 10^{-4}$	$3.589 \cdot 10^4$	1.584	0.974	0.547
0.005		$3.318 \cdot 10^{-4}$	$3.551 \cdot 10^4$	1.584	0.974	0.547
0.010		$3.685 \cdot 10^{-4}$	$3.178 \cdot 10^4$	1.589	0.974	0.545

TABLE VI. ΔQ dependence of the final results for a SW system: The parameters and notation coincide with those of tab. V, except for $\Delta \varrho = 5 \cdot 10^{-4} / \sigma^3$.

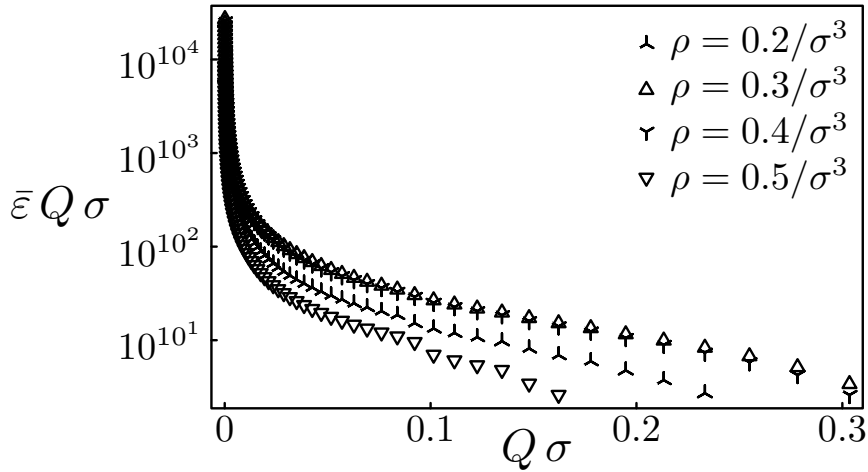


FIG. 1. $\bar{\epsilon} Q$ as a function of Q for various densities inside the binodal: The data have been obtained for a hard-core Yukawa potential with inverse screening length $z = 1.8/\sigma$ and for an inverse temperature of $\beta = 0.875/\epsilon$; the numerical precision in the calculations was $\epsilon_{\#} = 10^{-2}$, the step size for infinite cutoff was $\Delta Q|_{\infty} = 10^{-2}/\sigma$.

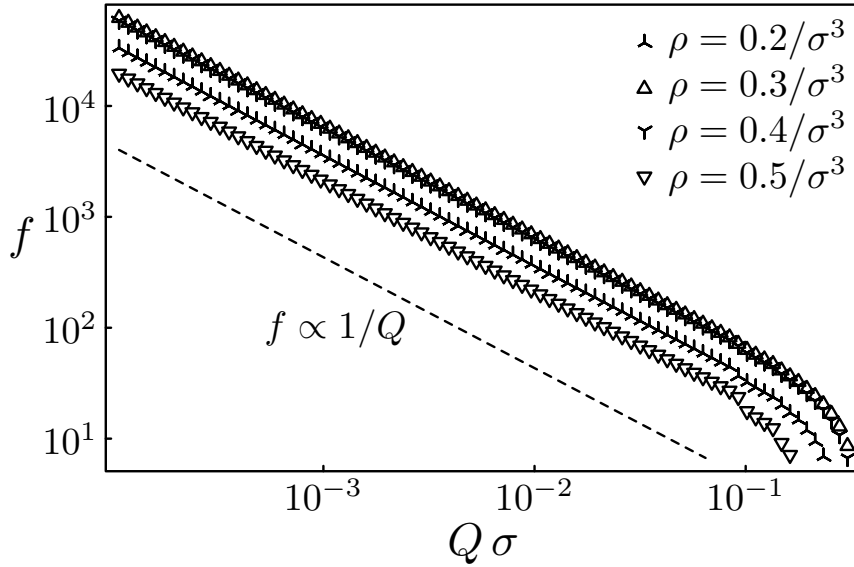


FIG. 2. f as a function of Q for various densities inside the binodal: The data have been obtained for the same hard-core Yukawa potential and with the same numerical parameters as in fig. 1. The dashed line indicates the slope corresponding to proportionality of f to the reciprocal of the cutoff; subsequent symbols are separated by ten steps in the $-Q$ direction.

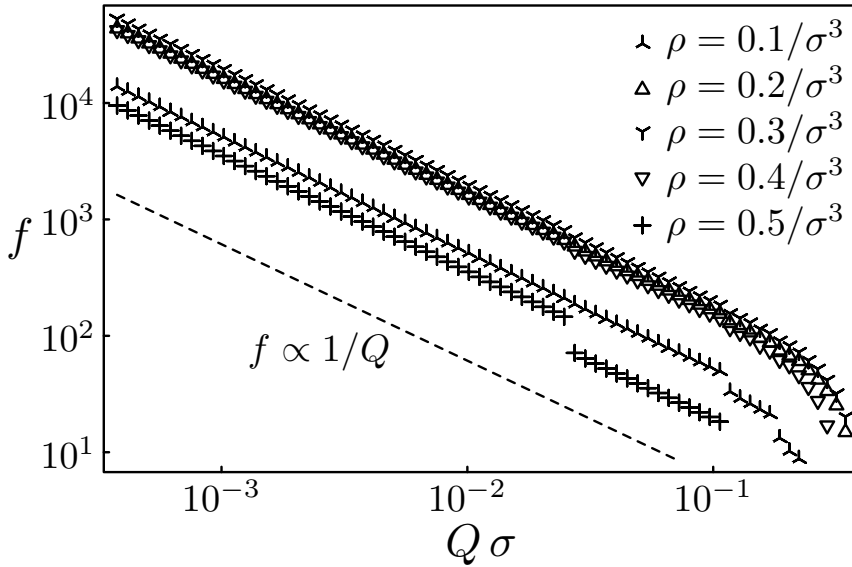


FIG. 3. f as a function of Q for various densities inside the binodal: The data have been obtained for a sw potential with $\lambda = 3$ and at a temperature of $\beta = 0.115/\epsilon$; otherwise, the remarks of fig. 2 apply.

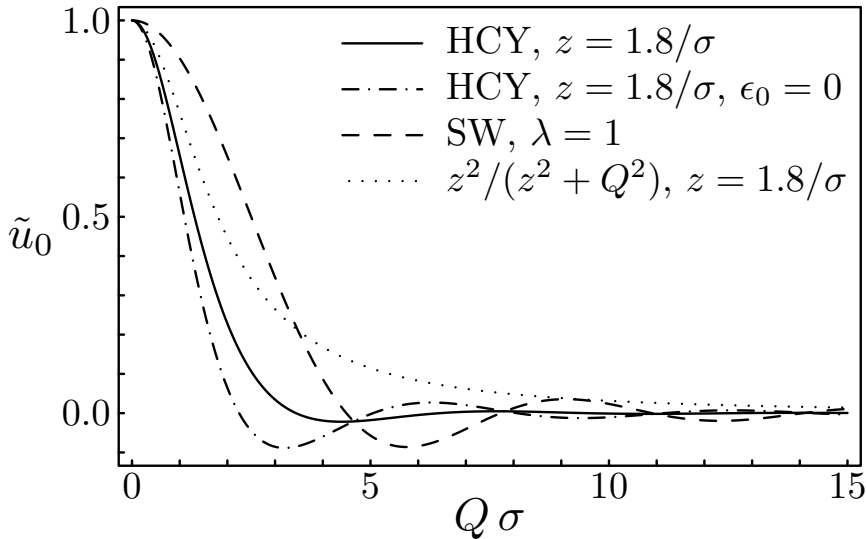


FIG. 4. \tilde{u}_0 as a function of Q for HCY and SW potentials with the parameters indicated; if, contrary to eq. (3), the Yukawa form is retained even inside the core, $\tilde{u}_0(Q)$ is given by $z^2/(z^2 + Q^2)$; as far as the SW potential is concerned, λ and Q enter \tilde{u}_0 only in the combination λQ so that a variation of the potential range only introduces a linear rescaling of the Q dependence of the function. We have checked that the graph remains qualitatively unchanged for different parameter settings. For reference, the first minimum of \tilde{u}_0 is -0.02 for the default HCY potential, -0.09 for the HCY potential with $\epsilon_0 = 0$, and slightly above -0.09 for the SW potential.

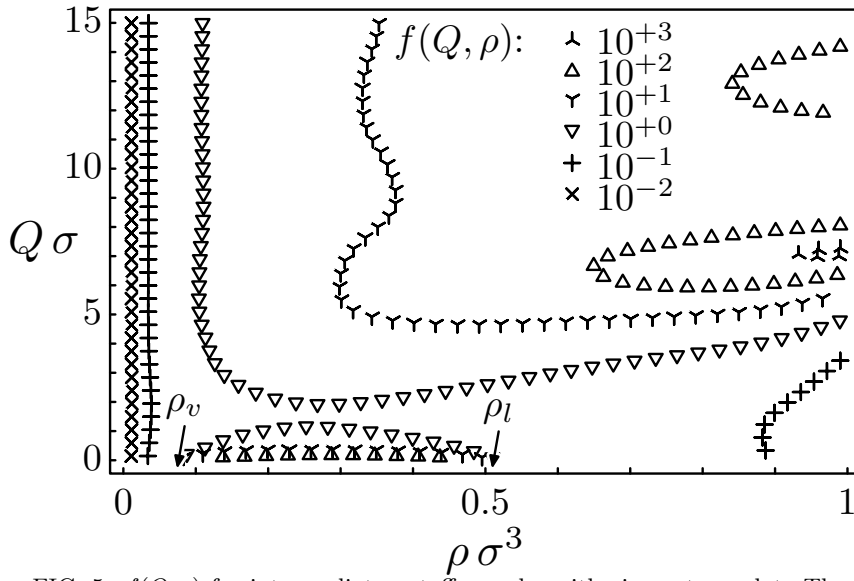


FIG. 5. $f(Q, \rho)$ for intermediate cutoff as a logarithmic contour plot: The data has been obtained for sws with $\lambda = 3$ at inverse temperature $\beta = 1/k_B T = 0.115/\epsilon$; both the approach to the low-density boundary condition of vanishing f at densities below $0.01/\sigma^3$ and the final build-up of infinite compressibility at cutoffs below $10^{-1}/\sigma$ have been excluded from the graph.